Influence of Elastic Deformation on Single-Wall Carbon Nanotube AFM Probe Resolution

Ian R. Shapiro, Santiago D. Solares, Maria J. Esplandiu, Lawrence A. Wade, William A. Goddard, and C. Patrick Collier**

Supporting Information

Tables of force field parameters:

TABLE 1: Force Field Energy Expression

Total Energy	$E = E_{\text{bond stretch}} + E_{\text{angle bend}} + E_{\text{torsion}} + E_{\text{stretch-bend-stretch}} + E_{\text{stretch-stretch}} + E_{\text{van der Waals}}$ *
Bond Stretch Energy Type Harmonic	$E = \frac{1}{2} K_b (R - R_o)^2$
Bond Stretch Energy Type Morse	$E = D_o (e^{-\alpha(R-R_o)} - 1)^2$ where $\alpha = \sqrt{\frac{K_b}{2D_o}}$

Angle Bend Energy Theta Harmonic	$E = \frac{1}{2} K_\theta (\theta - \theta_o)^2$
Angle Bend Energy Cosine Harmonic	$E = \frac{1}{2Sin^2\theta_o} K_\theta (Cos\theta - Cos\theta_o)^2$
Torsion Energy Dihedral	$E = \frac{1}{2} K_t [1 - d_t Cos(n_t \phi)]$
Stretch-Bend-Stretch Energy R-Cosine	$E = (Cos\theta - Cos\theta_o)[C_{ij}(Rij - Rij_o) + C_{jk}(Rjk - Rjk_o)]$
Stretch-Stretch Energy R-R	$E = K_{ss}(Rij - Rij_o)(Rjk - Rjk_o)$
Van der Waals Energy Morse	$E = D_o(\chi^2 - 2\chi)$ where $\chi = e^{\frac{-\gamma}{2}(\frac{R}{R_o} - 1)}$
Van der Waals Energy Lennard-Jones 6-12	$E = D_o((\frac{R_o}{R})^{12} - 2(\frac{R_o}{R})^6)$

* The present study did not consider charged samples or probes; hence the energy expression does not include electrostatic energy terms.

TABLE 2: Force Field Atom Types

H_	Non-acid hydrogen
H___A	Acid hydrogen
C_3	SP^3 carbon
C_2G	SP^2 graphite carbon
O_3	SP^3 oxygen
Si0	Bulk silicon
SiS	Surface silicon
SiOH	Surface silicon connected to OH group
SiH	Surface silicon connected to H_

TABLE 3: Harmonic Bond Stretch Parameters

Atom 1	Atom 2	K_b	R_o
SiOH	O_3	700.0000	1.5870
O_3	H___A	500.0000	1.0000
C_3	H_	662.6080	1.1094
C_3	C_3	699.5920	1.5140
C_2G	H_	700.0000	1.0200
C_2G	C_3	739.8881	1.4860
H_	H_	700.0000	0.7500

TABLE 4: Morse Bond Stretch Parameters

Atom 1	Atom 2	K_b	R_o	D_o
SiOH	H_	382.3870	1.4830	92.6000
SiH	H_	382.3870	1.4830	92.6000
Si0	Si0	193.0936	2.3810	73.7000
SiOH	Si0	193.0936	2.3810	73.7000
SiH	Si0	240.0660	2.3810	73.7000
SiOH	SiOH	193.0936	2.3810	73.7000
SiH	SiH	193.0936	2.3810	73.7000
C_2G	C_2G	720.0000	1.4114	133.0000
SiS	Si0	193.0936	2.3810	73.7000
SiS	SiS	193.0936	2.3810	73.7000

TABLE 5: Angle Bend Parameters

Atom 1	Atom 2	Atom 3	Type	K_θ	θ_o
C_2G	C_2G	C_2G	Cosine harmonic	196.1300	120.0000
C_2G	C_2G	C_3	Cosine harmonic	196.1300	120.0000
C_3	C_2G	C_3	Cosine harmonic	188.4421	120.0000
C_2G	C_3	C_2G	Cosine harmonic	220.2246	109.4710
C_3	C_3	C_3	Cosine harmonic	214.2065	109.4710
C_3	C_2G	H_	Cosine harmonic	98.7841	120.0000
Si0	SiH	H_	Cosine harmonic	42.2500	115.1400
Si0	Si0	Si0	Cosine harmonic	31.2682	105.0467
C_3	C_3	H_	Cosine harmonic	117.2321	109.4710
C_2G	C_3	H_	Cosine harmonic	121.6821	109.4710
C_2G	C_3	C_3	Cosine harmonic	220.2246	109.4710
C_2G	C_2G	H_	Cosine harmonic	103.1658	120.0000
Any	O_3	Any	Theta harmonic	100.0000	104.5100
H_	SiOH	H_	Cosine harmonic	58.2560	110.9530
Si0	SiOH	O_3	Cosine harmonic	102.7429	109.4710
SiOH	SiOH	Si0	Cosine harmonic	31.2682	105.0467
SiOH	Si0	Si0	Cosine harmonic	31.2682	105.0467
SiOH	Si0	SiOH	Cosine harmonic	31.2682	105.0467
SiH	SiH	Si0	Cosine harmonic	31.2682	105.0467
Si0	SiH	Si0	Cosine harmonic	31.2682	105.0467
SiH	Si0	SiH	Cosine harmonic	31.2682	105.0467
SiS	Si0	Si0	Cosine harmonic	31.2682	105.0467
SiS	Si0	SiS	Cosine harmonic	31.2682	105.0467
Si0	SiOH	Si0	Cosine harmonic	31.2682	105.0467
SiOH	SiOH	O_3	Cosine harmonic	102.7429	109.4710
SiH	SiH	H_	Cosine harmonic	42.2500	115.1400

Si0	SiS	Si0	Cosine harmonic	31.2682	105.0467
SiS	SiS	Si0	Cosine harmonic	31.2682	105.0467
O_3	SiOH	H_	Cosine harmonic	57.6239	109.4710

TABLE 6: Torsion Parameters

Atom 1	**Atom 2**	**Atom 3**	**Atom 4**	**K_t**	**n_t**	**d_t**
C_2G	C_2G	C_2G	C_2G	85.1200	2.0000	1.0000
Any	C_2G	C_2G	Any	100.0000	2.0000	1.0000
Any	C_2G	C_3	Any	2.0000	3.0000	-1.0000
Any	C_3	C_3	Any	2.0000	3.0000	-1.0000
Any	SiOH	O_3	Any	2.0000	3.0000	-1.0000

TABLE 7: Stretch-Bend-Stretch Parameters

Atom 1	**Atom 2**	**Atom 3**	**Rij**	**Rjk**	**θ_o**	**C_{ij}**	**C_{jk}**
Si0	Si0	Si0	2.3810	2.3810	109.4712	-14.8184	-14.8184

TABLE 8: Stretch-Stretch Parameters

Atom 1	**Atom 2**	**Atom 3**	**K_{ss}**	**Rij_o**	**Rjk_o**
Si0	Si0	Si0	3.6001	2.3810	2.3810

TABLE 9: van der Waals Parameters

Atom 1	**Atom 2**	**Type**	**D_o**	**R_o**	**γ**
H_	H_	Morse	0.018145	3.56979	10.70940

H___A	H___A	LJ 6-12	0.000099	3.19499	N/A
C_3	C_3	LJ 6-12	0.146699	3.98300	N/A
C_2G	C_2G	Morse	0.098999	3.993999	10.96300
O_3	O_3	LJ 6-12	0.095700	3.404599	N/A
Si0	Si0	LJ 6-12	0.310000	4.269999	N/A
SiS	SiS	LJ 6-12	0.310000	4.269999	N/A
SiOH	SiOH	LJ 6-12	0.310000	4.269999	N/A
SiH	SiH	LJ 6-12	0.310000	4.269999	N/A
C_2G	H_	Morse	0.034710	3.744610	12.25614
SiOH	C_2G	LJ 6-12	0.175186	4.132000	N/A
Si0	C_2G	LJ 6-12	0.175186	4.132000	N/A
SiH	C_2G	LJ 6-12	0.175186	4.132000	N/A
SiS	C_2G	LJ 6-12	0.175186	4.132000	N/A
O_3	C_2G	LJ 6-12	0.097336	3.699299	N/A

The original parameters used to create these force fields were developed in the Materials and Process Simulation Center (California Institute of Technology).[1,2,3] Additional parameters were added to study mixed systems (containing silicon, graphitic systems, oxygen and hydrogen) by applying arithmetic and/or geometric combination rules to existing parameters, by quantum mechanics calculations conducted by Weiqiao Deng, Richard Muller and William A. Goddard III or by using generic terms from the Dreiding force field.[4]

Energy-position and force-position curves from MD simulations:

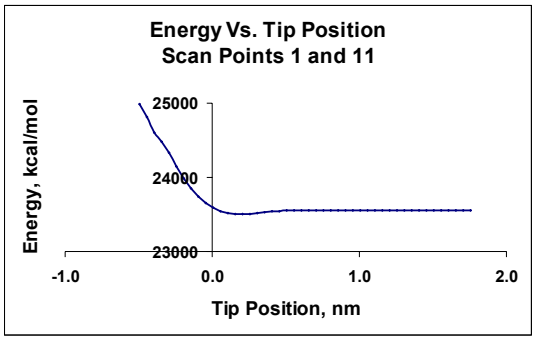

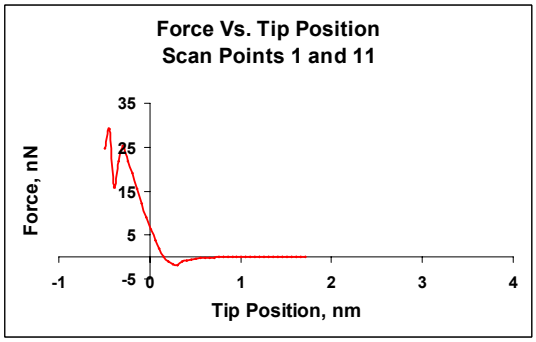

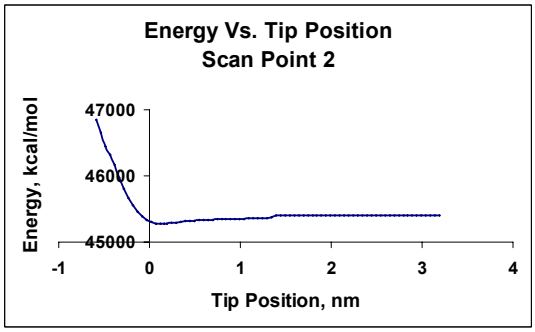

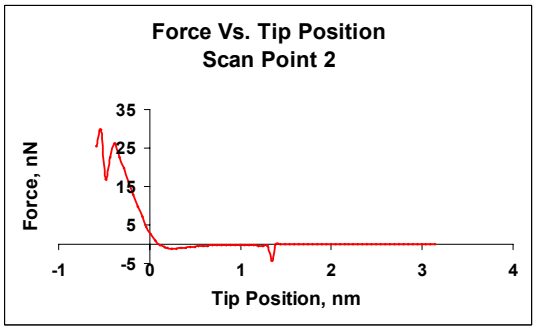

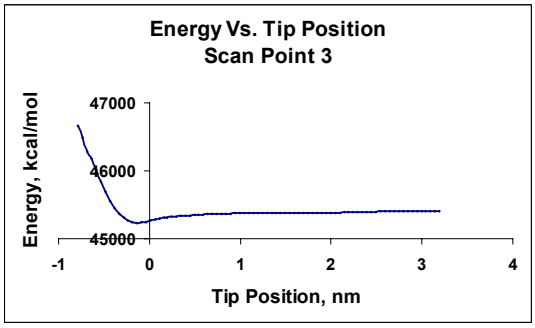

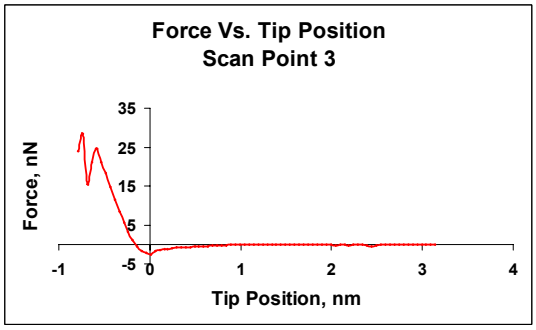

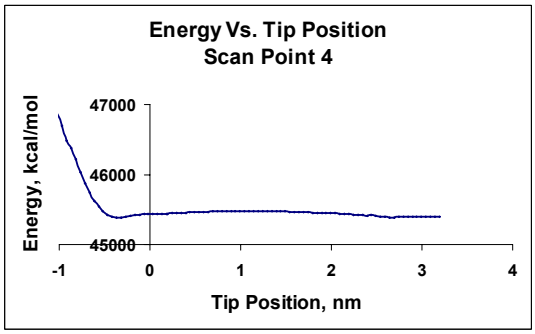

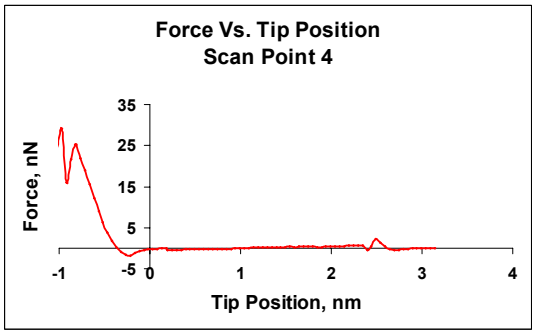

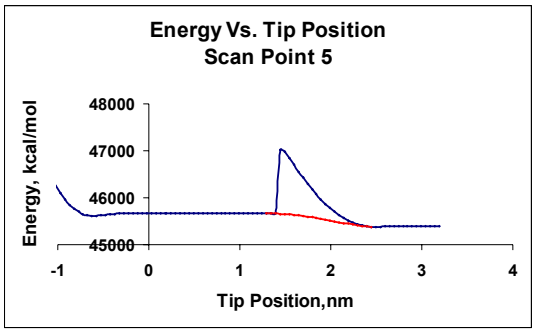
Energy Vs. Tip Position
Scan Point 5
Energy, kcal/mol
48000
47000
46000
45000
-1
0
1
2
3
4
Tip Position,nm

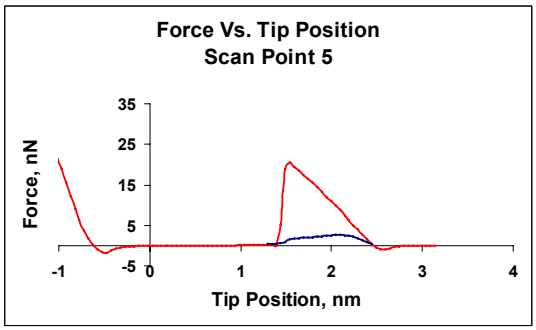
Force Vs. Tip Position
Scan Point 5
Force, nN
35
25
15
5
-5
-1
0
1
2
3
4
Tip Position, nm

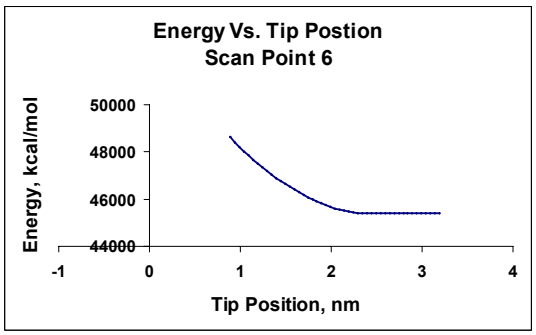
Energy Vs. Tip Postion
Scan Point 6
Energy, kcal/mol
50000
48000
46000
44000
-1
0
1
2
3
4
Tip Position, nm

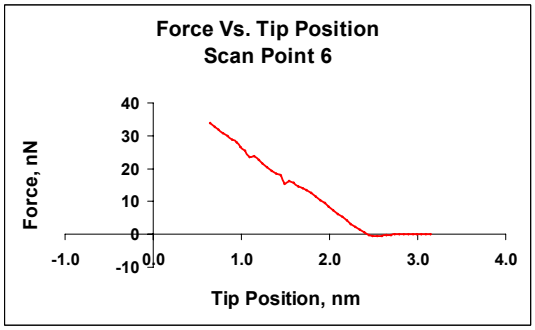
Force Vs. Tip Position
Scan Point 6
Force, nN
40
30
20
10
0
-10
-1.0
0.0
1.0
2.0
3.0
4.0
Tip Position, nm

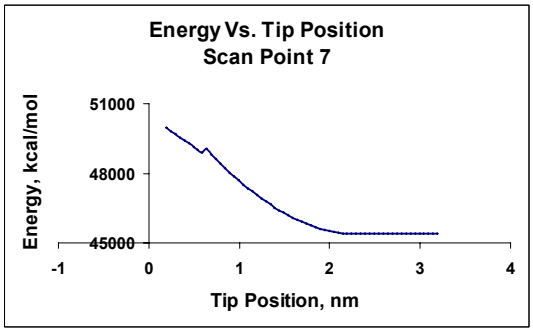
Energy Vs. Tip Position
Scan Point 7
Energy, kcal/mol
51000
48000
45000
-1
0
1
2
3
4
Tip Position, nm

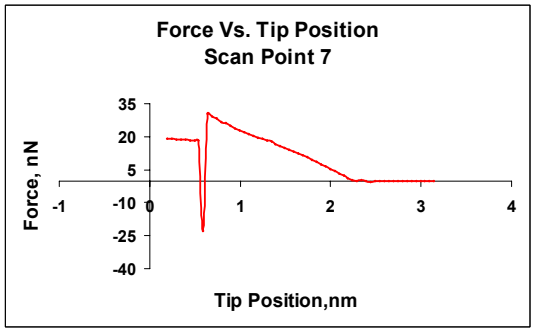
Force Vs. Tip Position
Scan Point 7
Force, nN
35
20
5
-10
-25
-40
-1
0
1
2
3
4
Tip Position,nm

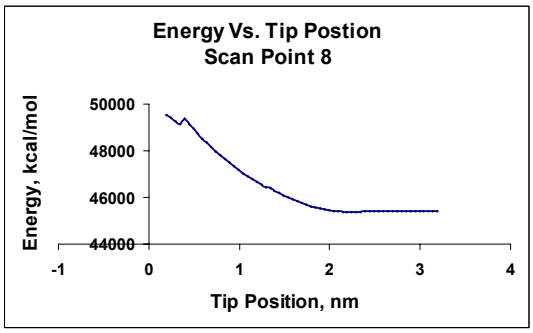
Energy Vs. Tip Postion
Scan Point 8
Energy, kcal/mol
50000
48000
46000
44000
-1
0
1
2
3
4
Tip Position, nm

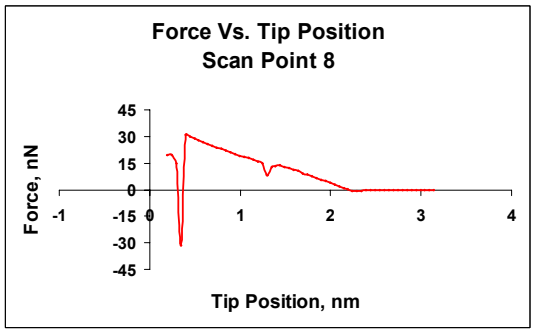
Force Vs. Tip Position
Scan Point 8
Force, nN
45
30
15
0
-15
-30
-45
-1
0
1
2
3
4
Tip Position, nm

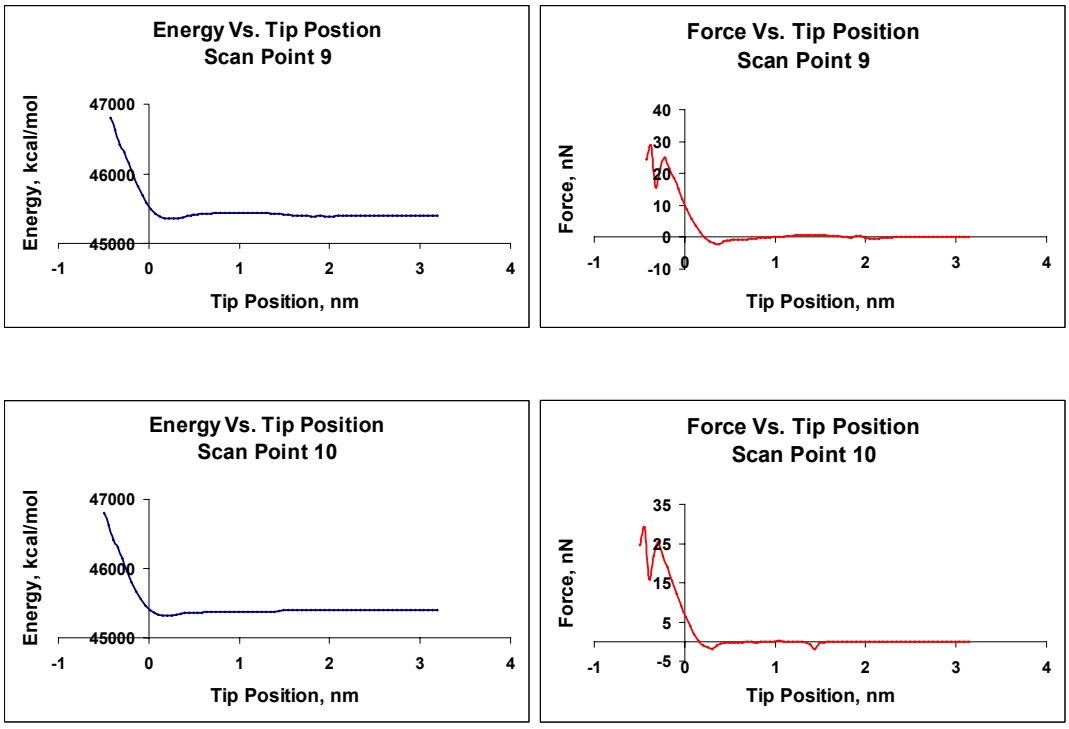

Figure S-1: Energy-distance and force-distance profiles generated for various probe positions, corresponding to the scan points in figure 2 of the manuscript.

Effect of thermal vibrations:

The tip-sample potentials and the corresponding force curves were constructed at zero kelvin to minimize the cost of the simulations. However, thermal vibration calculations at 300 K show that the potentials would not be significantly different at room temperature. The additional thermal energy would have the effect of lowering the energy barriers that the system needs to overcome in order for the probe to slip off the sample. This is only relevant for scan points 6, 7 and 8, for which the probe did not slip at the tip-sample forces present during tapping mode imaging. Only at much higher forces (~30 nN) did the probe slip off the sample nanotube at these points. The force and energy curves presented here show that the energy requirement to cause these points to slip is the same as that required to longitudinally compress the probe by one full nm, which is much greater than the available thermal energy. Our calculations show that the maximum horizontal displacement of any atom on the tip of the probe at 300 K is below 0.095 nm (less than 1.8% of the probe width), which would not significantly

change the relative position of probe and sample. The amplitude of the vertical vibrations is less than 0.055 nm.

Characterization of SWNT deformation modes:

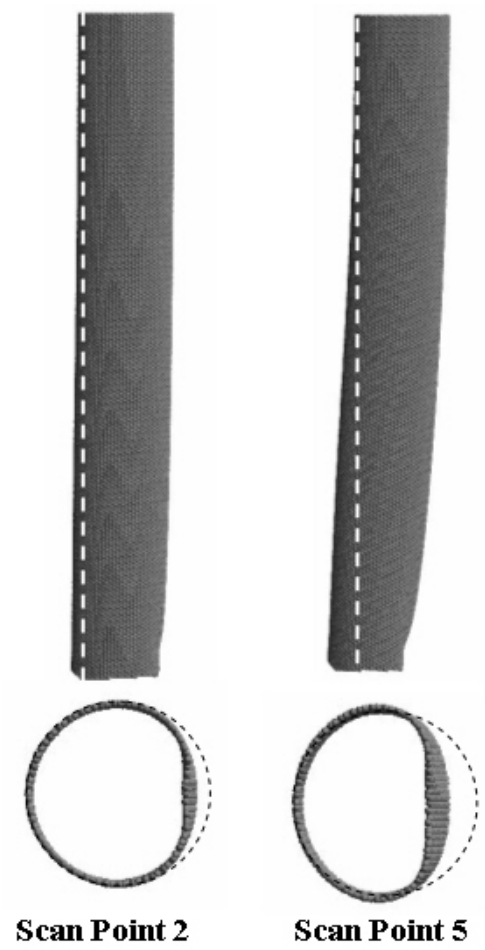

Figure S-2: Degree of probe bending shown for two extreme cases: scan point 2, the point on the scan where the 5.4 nm diameter probe nanotube first comes into contact with the sample nanotube, and scan point 5, the last point for which slipping occurred during the imaging simulation. The probe images have been rotated from their original tilted position to illustrate the amount of bending that the probe undergoes. The local deformation of the tip is also shown in the bottom pictures. The images show that both bending and local deformation contributes significantly to the reduction in the probe's effective resolution for this SWNT diameter.

Slipping of smaller SWNT probes: 2.2 nm diameter, 20 nm in length:

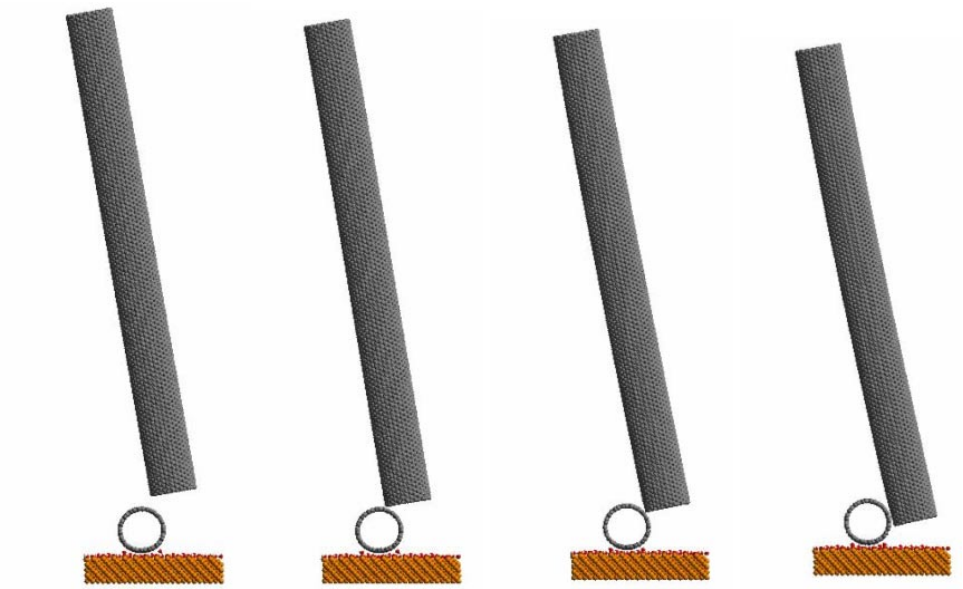

Figure S-3: The images from the simulation with the 2.2 nm diameter probe show that slipping also occurs for smaller probes, although it is primarily due to bending and not to local deformation, due to the higher radial stiffness for the thinner SWNT probes. In order to slip, the probe needed to displace laterally a distance of approximately 0.5 nm (22% of the sample diameter).

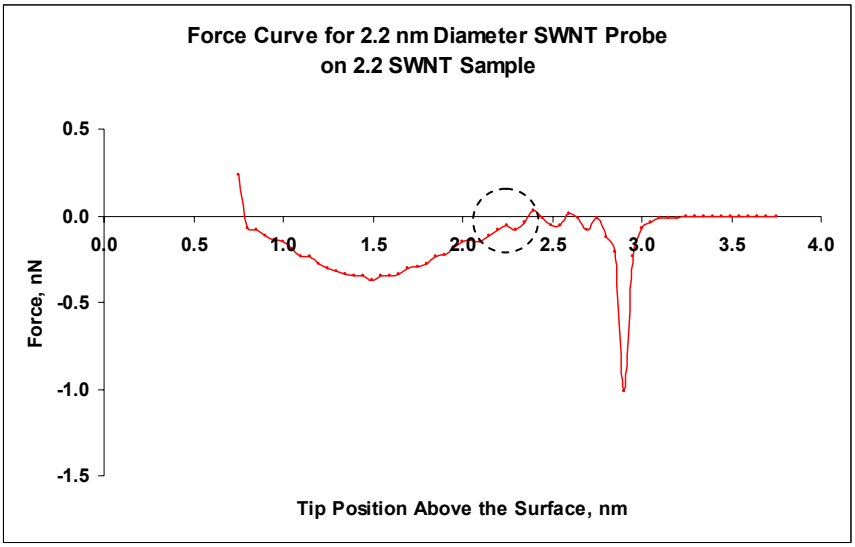

Figure S-4: Force curve for the 2.2 nm SNWT probe. The dashed circle shows the region where slipping occurs. As the graph shows, there is no significant force opposing the slipping motion of the probe. The negative peak in the force is due to snap-to-contact as the probe first approaches the sample.

Illustration of reversibility in SWNT probe-sample interaction:

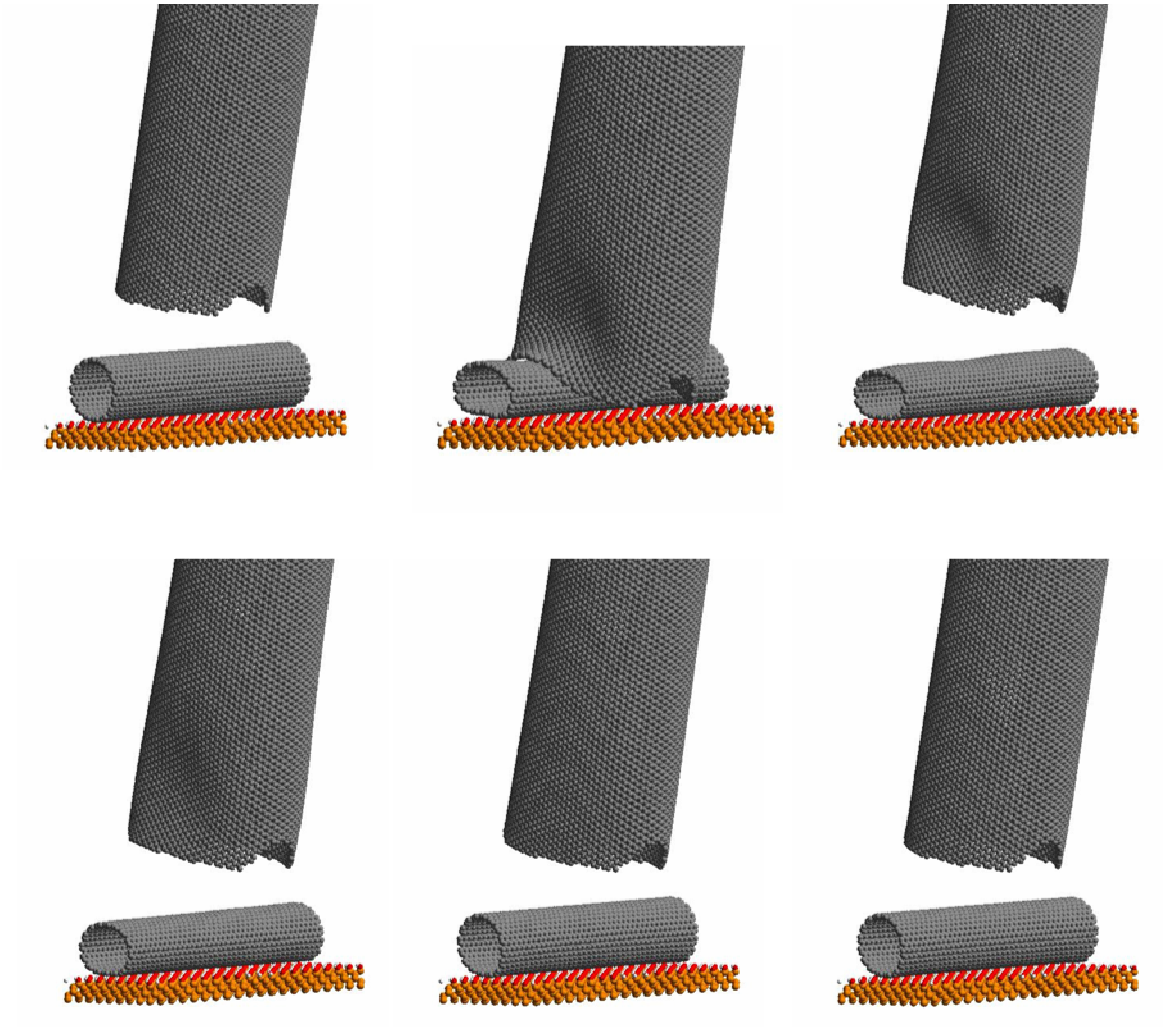

Figure S-5: Sequential images illustrating the reversible elastic nature of the deformation phenomenon. The top image on the left corresponds to the SWNT tip and sample before contact for scan point 6. The second image corresponds to the tip compressing the SWNT with a force of 33 nN (approximately twice the maximum tip-sample force observed during imaging). Images 3-6 correspond to intermediate geometry relaxation steps of the probe and sample after the probe has retracted. Note that the time required for geometry relaxation is on the order of 20 *ps,* one order of magnitude smaller than the integration time step used for AFM dynamics simulations (0.1 *ns*). This guarantees that the probe and sample are able to relax before the tip impacts the sample a second time.

References:

1. Musgrave, C.B., **1995.** PhD Dissertation Thesis: *"Molecular Mechanics and ab Initio Simulations of Silicon (111) Surface Reconstructions, Semiconductors and Semiconductor Superlattices, H Abstraction Tool for Nanotechnology, Polysilanes, and Growth of CVD Diamond"* California Institute of Technology.

2. Guo, Y.J. **1992.** PhD Dissertation Thesis: *"Molecular Simulations of Buckyball Fullerenes. Quantum Chemistry Studies on High Tc Superconductors"* California Institute of Technology.

3. Guo, Y.J.; Karasawan N.; Goddard W.A. III. *Nature,* **1991,** *351*, 6326.

4. Mayo, S.; Olafson, B.; Goddard, W. A. III. *J. Phys. Chem*. **1990**, 94, 8897.